MECHANICAL PROPERTIES OF NEW β-Ti ALLOY/CFRP BONDED STRUCTURE AT CRYOGENIC TEMPERATURES

Yohei Noji*, Tomohiro Yokozeki, Toshio Ogasawara***, Shinji Ogihara***
***Tokyo University of Science, **The University of Tokyo, ***Japan Aerospace Exploration Agency**

Keywords: *CFRP, Delamination, Adhesive, Titanium, Thermal stress, Thermal strain*

Abstract

This research investigated applicability of a new β-Ti alloy (Ti-36Nb-2Ta-3Zr-0.30, abbreviated as GM[TM]) developed in TOYOTA to metal-lined composite tanks for cryogenic propellant storage. Mechanical properties of cold-rolled GM plates, GM/GM and GM/CFRP adhesively bonded joints were evaluated at room and LN_2 temperatures. GM has superior strength and elastic deformation capability compared to conventional β-Titanium alloys as well as Al alloys. GM also exhibites low thermal expansion characteristic. Anisotropy characteristics in Young's modulus and coefficient of thermal expansion were observed. Modeling methodology for the elastic-plastic nonlinear behavior was proposed, and the nonlinear stress-strain behavior of GM was well-described using the proposed model. Fracture toughness of GM/CFRP adhesively-bonded joint was higher than that of A6061/CFRP bonded joint. It was demonstrated that GM has potential for a liner material of metal-lined composite tank for cryogenic propellant storage.

1 Introduction

Aluminum-lined carbon fiber composite (CFRP) pressure vessels are widely applied to hydrogen storage tanks of fuel-cell cars. The basic technology of Al-lined composite tanks has been established for gas hydrogen storage applications at room temperature. On the other hand, when an Al-lined composite tank is applied to cryogenic propellant storage, severe thermal stresses derived from significant CTE (coefficients of thermal expansion) mismatch between Al alloy and CFRP, leads to debondings between Al alloy and CFRP. Therefore, the development of cryogenic metal-lined CFRP tanks still remains a challenging technology. To establish cryogenic metal-lined CFRP tank technology, it is necessary to solve the debonding problem between CFRP and metal liner.

Recently, Saito et al. of TOYOTA (Toyota Central Research Institute, Japan) developed a new β-titanium alloy (Ti-36Nb-2Ta-3Zr-0.30) that has a super-elasticity such as low Young's modulus (averaged 40 GPa) and high elastic deformation capability (up to 2.5%), compared to the conventional β-Ti alloys such as Ti-15V-3Cr-3Sn-3Al [1]. Additionally, it is reported that the wire rod of this alloy has a small temperature dependency in elastic modulus (Elinvar behavior), a low CTE from cryogenic (-196℃) to high temperature (300℃) (Invar behavior), and excellent cold rolling processability.

Though these characteristics were confirmed in the cold-rolled wire rods, the properties of cold-rolled plates have not yet been acquired. Objective of this study is to evaluate the feasibility of the β-Ti alloy as the liner material, because the characteristics of a low Young's modulus and a low CTE and a high elastic deformation capability are preferable for preventing a metal lined tank from delamination problem.

This research investigates the mechanical behaviors of the β-Ti plates as a fundamental research of the development of metal-lined composite tanks for cryogenic propellant storage. Moreover, the strength and fracture characteristics of adhesively-bonded joints of the β-Ti are evaluated, and the results are compared with Al alloy adhesively-bonded joints.

2 Evaluation of Material Properties

2.1 Experimental Method

Cold rolled β-Ti alloy plates (*commercial name; Gum-metal* ^{TM}, abbreviated as GM in this paper) were supplied from Toyota Material Corporation, Japan. The nominal thickness (t) of the cold rolled plates was 0.1mm, 0.3mm, 0.5mm, and 1.0mm. The thickness of adhesively-bonded joint specimens was 3.0mm. Al alloy (A6061-T6) was also evaluated for comparison. The epoxy adhesive AF163-2K (3M, USA, t=0.2mm) was used for bonded joints.

2.1.1 Tension test

The specimen configuration is shown in Fig.1. The test method was referred to JIS Z 2201 (JIS; Japanese Industrial Standards). Specimens were cut from plates in the roll direction (L-direction) and the perpendicular direction (T-direction) in order to investigate anisotropy. The tensile loads were applied under constant displacement rate of 0.5mm/min. Residual strains were also measured by unloading the applied loads in every 0.3% strain step. A servo hydraulic-driven testing rig (8502, INSTRON, USA, loading cell 100kN) was used for tensile tests at room temperature. For tensile tests at LN_2 temperature, a mechanical-driven testing rig (4502, INSTRON, USA, loading cell 100kN) with a cryostat was used.

2.1.2 Evaluation of thermal expansion

Thermal expansion behaviors were evaluated using a laser interferometric dilatometer (LIX-1: ULVAC, Japan) from -150^{o}C to 200^{o}C. Specimens have 5mm width, 15mm length, and 1.0mm thickness. Three specimens were tested for CTE measurement in L- and T-directions, respectively.

2.1.3 Tension test of Single lap adhesively-bonded joints

The geometry and dimensions of a single-lap adhesively-bonded joint specimen is shown in Fig.2. The tension test was referred to JIS K 6850. The single-lap joint of Al alloy (A6061-T6) was also conducted for direct comparison. Specimens were bonded at 130^{o}C for 1 hr using a hot press according to a technical instruction of AF163-2K. Before the adhesion, surface treatments such as grind and etching were applied for both GM and A6061-T6.

The test speed was 0.2mm/min under the displacement control.

2.2 Results and Discussion

2.2.1 Tension test

A typical stress-strain curves of GM (t=1.0mm, L-direction, T-direction) are shown in Fig.3 (a) and (b). Nonlinear elastic behaviors are clearly observed from 0.8% to 1.1% with a slight hysteresis, and then plastic deformation appears above 1.1 %. The ultimate tensile strength and Young's modulus in the T-direction are slightly higher than those in the L-direction, and thus the anisotropy was confirmed.

Fig.4 shows the relationship between specimen thickness and Young's modulus. Young's modulus slightly increases with specimen thickness, and it was independent on temperature, and thus, so-called 'Elinvar' behavior was confirmed.

In order to understand the nonlinear behaviors, plastic onset strains were evaluated. A typical example of the relationship between residual strain and applied maximum strain is shown in Fig.5. Plastic onset strain was decided according to the following procedures.

1. A linearly approximated line is obtained from the residual strain data above 0.08% by linear regression, as indicated by red line in Fig.5.
2. The intersection point of the approximated line and the horizontal axis is defined as the plastic onset strain.

Fig.6 shows the relationship between specimen thickness and plastic onset strain. GM has higher plastic onset strain at cryogenic temperature compared to the case at room temperature. The plastic onset strain slightly increases with decrease in specimen thickness.

Considering the nonlinear behaviors and plastic onset strains, GM exhibits nonlinear elastic behaviors and plastic behaviors at room and cryogenic temperatures. For example, GM with 1mm thickness exhibited clear nonlinear behaviors below 1% strain at room temperature, but the plastic onset strain was estimated to be about 1.5%. Therefore, it was concluded that GM exhibits nonlinear behaviors which consist both of elastic and plastic nonlinearity.

The mechanical properties of GM, A6061-T6 and a typical β-Ti alloy (Ti-15V-3Cr-3Sn-3Al) are summarized in Table 1 and Table 2. GM exhibits much higher 0.2% yield stress and tensile strength as compared with the conventional β-Ti alloy as well as

A6061-T6, and thus, excellent elastic deformation capability. These properties are preferable for liner materials of cryogenic propellant tanks.

2.2.2 Thermal expansion

The coefficient of thermal expansion (CTE) was determined by derivation of the thermal expansion data. Fig. 7 shows CTEs of GM from 150ºC to 180ºC. The CTEs of GM, A6061-T6 and a typical β-Ti alloy at 23ºC are summarized in Table 1, and Table 2.

GM exhibited significant anisotropic CTEs in L- and T-directions. The CTE in L-direction is approximately a half of that in T-direction, whereas the CTE in T-direction is almost same as that of the conventional β-Ti alloy. It is considered that the low CTE in L-direction is due to its characteristic microstructure derived from a cold rolling process.

2.2.3 Tension test of Single lap adhesively-bonded joints

The experimental results of adhesive shear strengths are shown in Table 3. GM/GM bonded joint exhibits higher shear strength than those of Al/Al bonded joint at LN_2 temperature, whereas GM/GM and Al/Al have similar adhesive shear strength at room temperature.

The fracture surfaces were observed by an optical microscope. Both single-lap joint specimens of GM and Al alloy were broken in the adhesive layer at room temperature, which shows that the shear strength of the interface is higher than that of the adhesive. On the other hand, both GM and Al alloy bonded specimens were broken at the interface between the metal and the adhesive at LN_2 temperature. It was demonstrated that GM/GM bonded joint has superior adhesive strength compared to Al/Al bonded joint within the cases of the selected adhesives (AF163-2K).

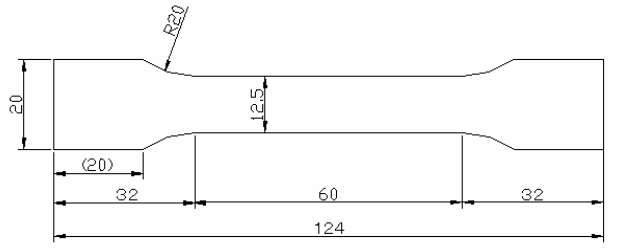

Fig.1 Geometry and dimension of tensile test specimen (t=0.1, 0.3, 0.5, 1.0)

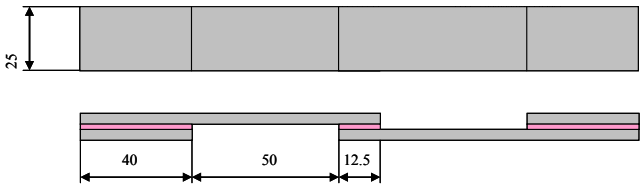

Fig.2 Geometry and dimension of single lap adhesively-bonded joint specimen (t=3.0)

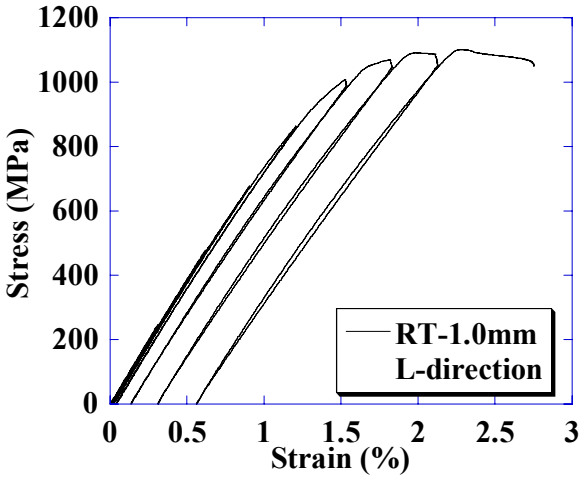

(a) L-direction, t=1mm

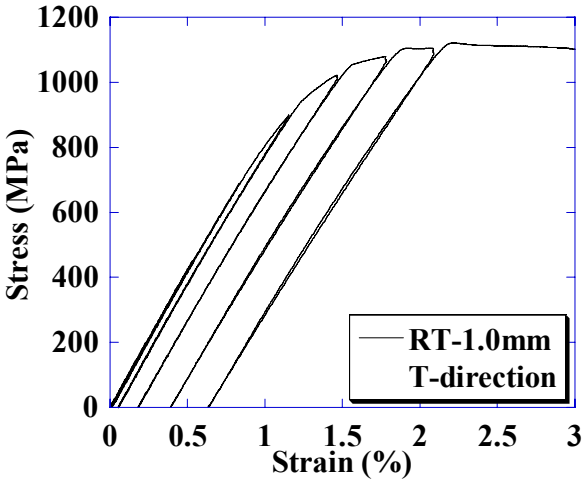

(b) T-direction, t=1mm

Fig.3 Stress-Strain curve of GM obtained by loading-unloading tests at room temperature

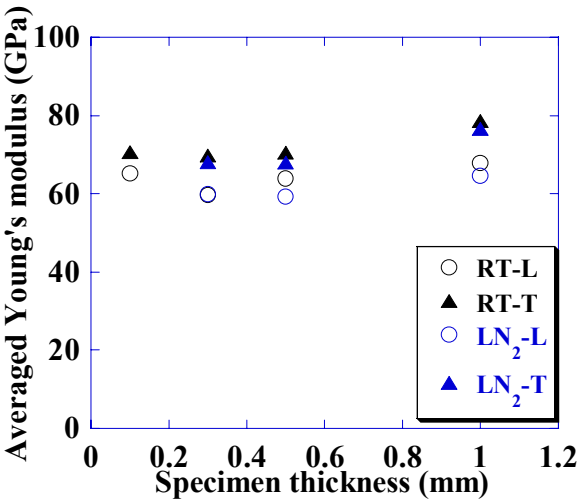

Fig.4 Relationship between Young's modulus and specimen thickness

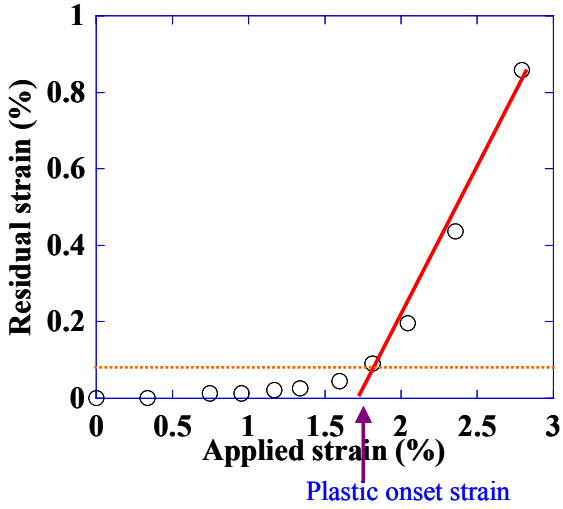

Fig.5 Definition of plastic onset strain in applied strain versus residual strain.

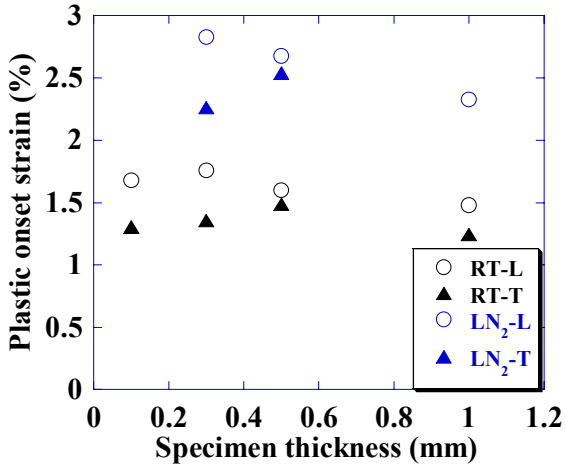

Fig.6 Relationship between plastic onset strain and specimen thickness

Table1 Material properties of GM (t=1.0mm)

Material	GM (Ti-36Nb-2Ta-3Zr-0.30)			
Direction	L		T	
Temperature [℃]	23	-196	23	-196
Young's modulus [GPa]	67.9	64.5	78.7	76.6
Tensile strength [MPa]	1103	-	1124	-
0.2% proof strength [MPa]	1024	1684	1014	1627
CTE [10^{-6}/℃]	4.7	-	9.1	-

Table2 Material properties of typical β-Ti and Al alloy (A6061-T6)

Material	β-Ti alloy*[2]		Al alloy**[3]	
Temperature [℃]	23	-196	23	-196
Young's modulus [GPa]	82	-	69.8	77.1
Tensile strength [MPa]	790	-	311	-
0.2% proof strength [MPa]	781	-	282	311
CTE [10^{-6}/℃]	8.5	-	18.2	-

* Ti-15V-3Cr-3Sn-3Al
** A6061-T6

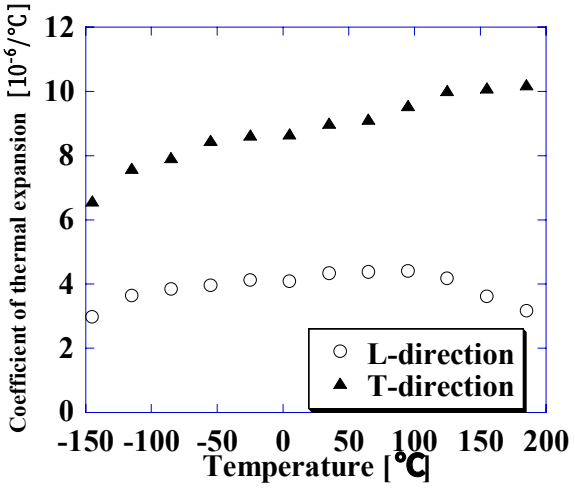

Fig.7 Coefficient of thermal expansion (CTE) of GM (t = 1mm)

Table3 Shear adhesive strength of single-lap joints (adhesive AF163-2K)

Temperature	Shear strength (MPa)	
	GM/GM	A6061/A6061
RT	25.23 (0.44)	22.31 (1.77)
LN_2	26.01 (2.19)	11.37 (2.57)

( ): standard deviation

3. Modeling of Nonlinear Behavior for GM

Modeling of nonlinear elastic/plastic behavior of GM observed in the tension tests is presented in this section, because accurate model is necessary to simulate the delamination progress of a lined-tank structure. The model proposed here is verified by comparison with experimental results.

3.1 Nonlinear Constitutive Equation

The experimental results suggested that GM exhibited elastic and plastic nonlinear behaviors. Therefore, the present model consists of a nonlinear elastic model and a plastic model. The experimental strains were divided into the elastic strain and the plastic strain from the experimental stress-strain curves with plastic onset strain evaluated in section 2.2.1.

3.1.1 Nonlinear elastic model

Hahn and Tsai [4] proposed a constitutive equation derived from higher order strain energy functions for representing a nonlinear shear behavior of unidirectional composite material. Ishikawa et al. expanded this model to nonliniear on-axis elastic behavior of unidirectional composite materials [5]. Here, this idea is adopted for the description of the nonlinear elastic behavior of GM, because GM exhibits anisotropy and nonlinear elastic behaviors. L- and T-direction is denoted as 1- and 2-directon, respectively, in the following formulation. According to Hahn and Tsai, the strain energy function of an orthotropic material is assumed to be expressed as forth-order polynomials of stress. When following conditions are assumed;

1) Plane stress state
2) No coupling of σ_1 and σ_2 in a nonlinear term of strain energy.
3) No coupling of shear stresses and normal stresses in strain energy.

Complemental strain energy under unidirectional stress parallel to 1-direction is expressed as

$$W_c = \frac{1}{2}S_{11}\sigma_1^2 + \frac{1}{2}S_{22}\sigma_2^2 + \frac{1}{2}S_{66}\sigma_6^2 + S_{12}\sigma_1\sigma_2 + \frac{1}{3}S_{111}\sigma_1^3 + \frac{1}{3}S_{222}\sigma_2^3 + \frac{1}{4}S_{1111}\sigma_1^4 + \frac{1}{4}S_{2222}\sigma_2^4 + \frac{1}{4}S_{6666}\sigma_6^4 \quad (1)$$

Then, strain can be obtained by differentiating the complemental strain energy with respect to stress as follows;

$$\varepsilon_{ij} = \frac{\partial W_c}{\partial \sigma_{ij}} \quad (2)$$

The relationship between the elastic strain and the stress is given by

$$\begin{Bmatrix} \varepsilon_1^e \\ \varepsilon_2^e \\ \gamma_{12}^e \end{Bmatrix} = \begin{bmatrix} S_{11}+S_{111}\sigma_1+S_{1111}\sigma_1^2 & S_{12} & 0 \\ S_{12} & S_{22}+S_{222}\sigma_2+S_{2222}\sigma_2^2 & 0 \\ 0 & 0 & S_{66}+S_{6666}\tau_{12}^2 \end{bmatrix} \times \begin{Bmatrix} \sigma_1 \\ \sigma_2 \\ \tau_{12} \end{Bmatrix} \quad (3)$$

Experimental elastic stress-strain relation was approximated by the quadratic function using equation (3) to obtain the nonlinear elastic properties. Parameter S_{66} was not able to be decided because of no examination in the direction of 45° within this study. This term was neglected, which was further to be investigated.

3.1.2 Plastic model

In order to account for anisotropic plastic behaviors, the Hill's plastic potential [6] was utilized for the plastic response model.

$$2f(\sigma_{ij}) \equiv F(\sigma_2-\sigma_3)^2 + G(\sigma_3-\sigma_1)^2 + H(\sigma_1-\sigma_2)^2 + 2L\tau_{23}^2 + 2M\tau_{31}^2 + 2N\tau_{12}^2 \quad (4)$$

The effective stress and the effective plastic strain are expressed as the following equations when subjected to uniaxial loading with off-axis angle θ to the longitudinal axis (1-direction) [7].

$$\bar{\sigma} = \sigma_x \sqrt{\frac{3}{2}\left(\cos^4\theta + a_{22}\sin^4\theta + (a_{66}-1)\cos^2\theta\sin^2\theta\right)} \equiv \sigma_x h(\theta) \quad (5)$$

$$d\bar{\varepsilon}^p = \frac{d\varepsilon_x^p}{h(\theta)}, \quad \bar{\varepsilon}^p = \frac{\varepsilon_x^p}{h(\theta)} \tag{6}$$

Especially, when GM is subjected to uniaxial loading in 1-direction, the following equations are obtained.

$$\bar{\sigma} = \sqrt{\frac{3}{2}}\sigma_x, \quad \bar{\varepsilon}^p = \sqrt{\frac{2}{3}}\varepsilon_x^p \tag{7}$$

Similarly, when GM is subjected to uniaxial loading in 2-direction, the effective stress and effective plastic strain are given by

$$\bar{\sigma} = \sqrt{\frac{3}{2}a_{22}}\sigma_x, \quad \bar{\varepsilon}^p = \sqrt{\frac{2}{3a_{22}}}\varepsilon_x^p \tag{8}$$

Based on the above expressions, the relation of effective stress-effective plastic strain can determined using the experimental results. In order to obtain a master curve of the effective stress-effective plastic strain relation, the following power law is applied

$$\bar{\varepsilon}^p = A\bar{\sigma}^n \tag{9}$$

In this model, parameter a_{22} is decided by fitting of the obtained curve based on the experimental data.

3.2 Results and Discussions

The nonlinear elastic behaviors were evaluated based on the present modeling, and the elastic parameters of each GM specimen (with different thickness) were obtained at room and cryogenic temperatures. In the case of the plastic behavior, parameter a_{22} was decided so that the obtained effective stress-effective plastic strain curves collapse into a single curve that does not depend on thickness and loading direction. The obtained parameter a_{22} was 1.045 at the room temperature and 1.185 at LN_2 temperature. Because these parameters were close to 1, it can be considered that the plastic behaviors of GM are regarded as isotropic.

The relationship between effective stress and effective plastic strain is shown in Fig.8 when the parameter a_{22} is set to be 1. In this case, it can also be confirmed that effective stress-effective plastic strain curve doesn't depend on thickness and loading direction. The predicted stress-strain curves using the obtained parameters (elastic parameters and a_{22}) are compared with the experimental curves. A typical result is shown in Fig.9, which indicates that the predicted curve agrees well with the experiment results. It is demonstrated that nonlinear behaviors of GM (including elastic and plastic behaviors) can be well-described using the present modeling.

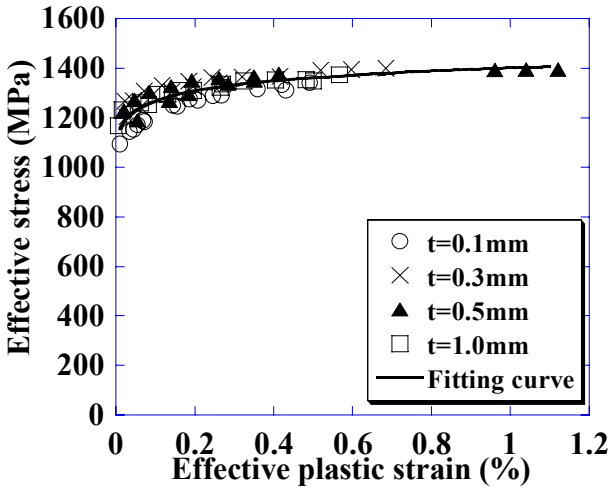

Fig.8 Effective stress-effective plastic strain curve of GM at room temperature (a_{22} = 1).

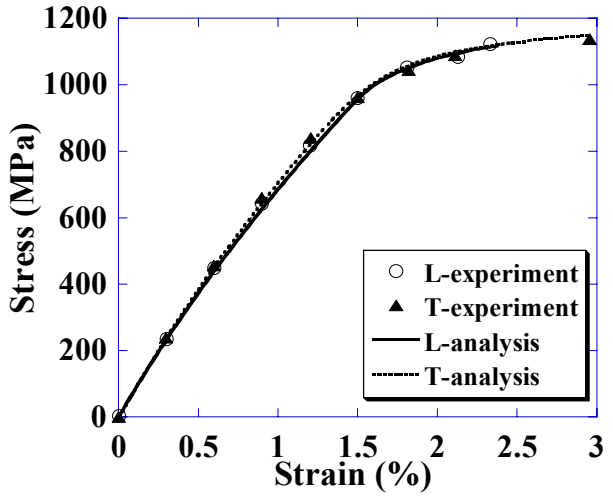

Fig.9 Comparison between experimental result and analytical prediction at room temperature (t=0.5mm)

4. Fracture Toughness Evaluation of GM/GM and GM/CFRP Adhesively Bonded Joints

Fracture toughness of GM/GM and GM/CFRP adhesively-bonded joints was measured using Double Cantilever Beam (DCB) at room and LN_2 temperatures. Apparent Mode I fracture toughness (G_c) of GM/ GM and GM/CFRP bonded joints were measured. A6061-T6/CFRP bonded joint was also evaluated for direct comparison.

4.1 Experimental Method

4.1.1 Specimen

GM/GM, GM/CFRP and A6061-T6/CFRP adhesively-bonded joint specimens were prepared. The thickness of GM, A6061-T6, and CFRP was 3.0mm, 3.0mm, and 2.0 mm, respectively. CFRP used in this study was MR50K/#1063EX (Mitsubishi rayon, Japan). Two kinds of layup laminates, quasi-isotropic layup, $[45/0/-45/90]_{2S}$, (denoted as QI) and unidirectional layup, $[0]_{16}$, were used for GM/CFRP joints, whereas only quasi-isotropic layup, $[45/0/-45/90]_{2S}$ was used for A6061-T6/CFRP. The resultant volume fraction was 62%. The adhesive was AF163-2K (3M, USA, t=0.2mm), which is the same adhesive used in single-lap joint tension test. The surface treatment was applied to GM, A6061-T6, and CFRP respectively according to the technical instruction of AF163-2K prior to adhesion. Release films were inserted between the adherend and the adhesive as a crack starter. The specimen configuration is shown in Fig.10.

4.1.2 Experimental method

DCB tests at room temperature were conducted using a mechanical-driven testing rig (4502, INSTRON, USA; load cell-5kN) according to JIS K 7086. Loads were applied under a constant displacement rate (0.5 mm/min), and the test machine was stopped whenever crack growth of more than 5mm was observed. Then, the actual crack length was visually measured, followed by unloading operation to obtain the compliance of the specimen. The above-mentioned operations were repeated seven times.

DCB tests at LN_2 temperature were conducted using the test machine used in the previous tension test at LN_2 temperature. In the case of cryogenic DCB test, two crack gauges (Fig.11) were attached in series on each side of a specimen because the crack length was not able to be visually measured during DCB test.

Adhesive fracture toughness of bonded specimens was evaluated using a corrected compliance method as indicated in JIS K 7086.

4.2 Results and Discussions

4.2.1 GM/GM adhesively bonded joints

The fracture toughness of GM/GM and CFRP/CFRP adhesively bonded joints are shown in Table 4. When the fracture surfaces were observed after the test, adhesives remained on both sides of separated specimens at room temperature, which indicates the adhesive fracture (crack growth in the adhesive layer), whereas the delamination at the interface between the adhesive and the adherend was observed at LN_2 temperature. It is thought that the crack progressed in the adhesive because the fracture toughness associated with interface crack growth is larger than that associated with crack growth in the adhesive layer at room temperature.

4.2.2 GM/CFRP adhesively bonded joints

The experimental results of fracture toughnesses were compared as shown in Table 5. When the fracture surfaces were observed after the test, it was confirmed that the crack progressed in the adhesive layer at room temperature for GM/CFRP bonded joints (the cases both of QI and UD). It can be said that fracture toughness associated with interface crack growth is higher than that associated with crack growth in the adhesive layer. At LN_2 temperature, the crack path shifts from the interface between the adherend and the adhesive to the inner layer of CFRP, when the crack grows by 2mm in both GM/CFRP(QI and UD) and A6061-T6/CFRP adhesively-bonded joints. Therefore, the adhesive fracture toughness was evaluated using the data corresponding to the first crack growth in this study.

GM/CFRP(QI) bonded joint exhibited the 34% higher fracture toughness than A6061-T6/CFRP bonded joint, though fracture toughness decreased by about 33% at LN_2 temperature compared to that at room temperature. This is due to small difference of CTE between GM and CFRP. The experimental results suggest that GM has a potential for the liner material of composite tank structures.

5. Conclusion

Mechanical properties of cold-rolled GM plates, GM/GM and GM/CFRP adhesively bonded joints were evaluated at room and LN_2 temperatures in order to investigate the applicability to metal-lined cryogenic composite tanks. The following conclusions were made:

1. GM has superior strength and elastic deformation capability compared to conventional β-Titanium alloy as well as Al alloy. Moreover, GM also exhibited low thermal expansion characteristic in rolling direction and good adhesively bonded strength.
2. GM has anisotropy characteristics in Young's modulus and coefficient of thermal expansion. Modeling methodology for the elastic-plastic nonlinear behavior was proposed, and the nonlinear stress-strain behavior was well-described using the proposed model.
3. Mode I fracture toughness of GM/CFRP adhesively-bonded joints was higher than that of A6061/CFRP bonded joints.
4. It was demonstrated that GM has potential for a liner material of metal-lined composite tank for cryogenic propellant storage as compared with Al alloy.

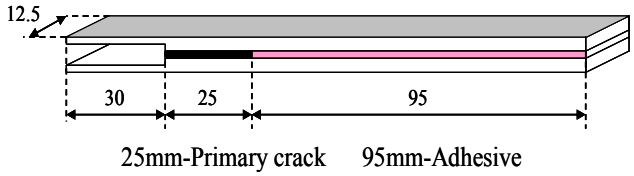

Fig.10 Geometry and dimension of DCB test specimen

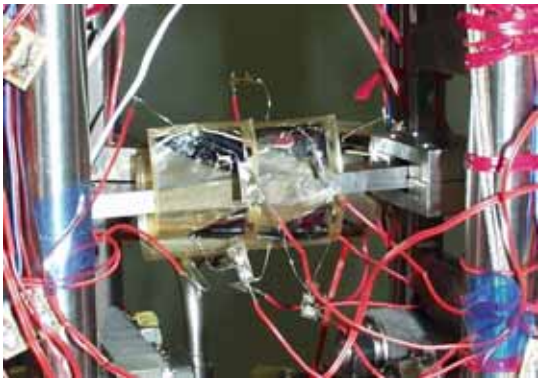

Fig.11 Crack gauges

Table4 Mode I fracture toughness G_C of GM/GM and CFRP/CFRP adhesively bonded joints.

Temperature	Fracture toughness G_C [kJ/m^2]	
	GM/ Adhesive /GM	CFRP/ Adhesive /CFRP[8]
RT	1.69 1.65 1.73	1.80
-150℃	-	0.52
LN_2	0.46 0.22	-

Table5 Mode I fracture toughness G_C of GM/CFRP and A6061/CFRP adhesively bonded joints.

Temperature	Fracture toughness G_C [kJ/m^2]		
	GM/ /CFRP(QI)	GM/ /CFRP(UD)	Al alloy/ /CFRP(QI)
RT	2.63	1.98 2.53	-
LN_2	1.76	1.83 2.80	1.31

References

[1] T. Saito et al, Multifunctional Alloys Obtained via a Dislocation-Free Plastic Deformation Mechanism, Science, 300, p464-467 (2003)
[2] http://www.matweb.com/
[3] R. Maruyama, Applicability evaluation of SiC-FRP to cryogenic liner tank structures, Graduation thesis, Aoyama Gakuin Univ. (2005)
[4] T. Hahn and S. W. Tsai, Nonlinear Elastic Behavior of Unidirectional Composite Lamina, Journal of Composite Materials, Vol.7 (1973)
[5] T. Ishikawa et al., Longitudinal Material Nonlinear Properties of Unidirectional Carbon Composites, The Japan Society for Composite Materials, 12,1 (1986), p8-15
[6] Hill.R, The Mathematical Theory of Plasticity, Oxford University Press, London (1950)
[7] C. T. Sun and J. L. Chen, A Simple Flow Rule for Characterizing Nonlinear Behavior of Fiber Composites, J. Comp. Mater., Vol.23, p1009-1020, 1989
[8] anmei HE et al,Temperature-dependent Fracture Behavior of CFRP-Film Adhesive Bond Joints, Proceedings of the 29th Symposium on Composite Materials, p163-164 (2004)